GEOSMART

Project acronym:	GeoSmart		
Project title:	Technologies for geothermal to enhance competitiveness in smart and flexible operation		
Activity:	LC-SC3-RES-12-2018		
Call:	H2020-LC-SC3-2018-RES-SingleStage		
Funding Scheme:	IA	Grant Agreement No:	818576
WP 4	Development of scaling reduction system		

D4.5 Report on design and building of retention tank

Due date:	30/09/2021 (M28)	
Actual Submission Date:	07/10/2021	
Lead Beneficiary:	Spike Renewables Srl	
Main authors/contributors:	Paolo Taddei Pardelli, Claretta Tempesti, Andrea Mannelli, Alex Sabard, Briony Holmes	
Dissemination Level[1]:	PU	
Nature:	REPORT	
Status of this version:		Draft under Development
		For Review by Coordinator
	X	Submitted
Version:	2	
Abstract	GeoSmart aims to develop a solution based on retention system technology to control and reduce the silica scale formation before re-injection to fully utilize the thermal energy of a well.	

REVISION HISTORY

Version	Date	Main Authors/Contributors	Description of changes
1	08/09/2021	P.Taddei Pardelli / C.Tempesti / A.Mannelli	Initial version
2	23/09/2021	P.Taddei Pardelli / C.Tempesti / A.Mannelli	Update
3	04/10/2021	P.Taddei Pardelli / C.Tempesti / A.Mannelli	Final version with Partners comments

---

[1] Dissemination level security:

PU – Public (e.g. on website, for publication etc.) / **PP** – Restricted to other programme participants (incl. Commission services) /

RE – Restricted to a group specified by the consortium (incl. Commission services) / **CO** – confidential, only for members of the consortium (incl. Commission services)

Document: D4.5 Report on design and building of retention tank

Version: 2.0

Date: 7 October 2021

CONTENTS

Acronyms

Ar	Argon
ASTM	American Society for Testing and Materials
DPI	Dye penetrant inspection
KPI	Key performance indicator
P&ID	Piping and instrumentation diagram
SCC	Stress corrosion cracking
TIG	Tungsten Inert Gas
WPS	Welding Procedure Specification

Summary

The current deliverable details the **Retention tank design for construction** for GeoSmart project. This system will be developed and tested to address one of the main challenges of GeoSmart project i.e. reducing the reinjection temperature of geothermal brine: a limiting constraint to fully utilising the thermal energy of a well is often the need to reinject geothermal brine at high enough temperature to prevent fouling. Thanks to the retention system the scaling can drastically be reduced and the lower reinjection temperature can produce more energy and increase overall geothermal plant efficiency.

GeoSmart indeed aims to develop a solution based on retention system technology to control and reduce the silica scale formation before re-injection. Lowering reinjection temperature would strongly increase plant efficiency by providing extra useful heat. Based on silica scaling numerical simulation, the effects of parameters like pH, temperature and brine composition on silica polymerization and scaling deposition rates have been evaluated and the design and optimization of the retention system has been developed.

At the inlet of the retention system there will be brine at 50°C coming from the heat exchanger: in these conditions, silica scaling formation can occur after a certain amount of time. The Retention Tank system is composed by n.2 tanks: **the scaling reactor** ($10m^3$) where silica scaling is encouraged (in order to enable mineral extraction) by modifying the pH to 8.5 and **the Retention Tank** ($10m^3$) where silica polymerization is encouraged by lowering the pH at 5.0. In fact, it is necessary to avoid scaling downstream of the RT in the reinjection into the well as it would block the whole system. The retention tank has been designed and developed so that the scaling deposits will occur inside the device; the dimensioning has taken into account the results obtained in previous studies conducted by the University of Iceland (UOI) related to Silica scaling modelling and inhibitors. The system will be tested at Zorlu's Kızıldere-II geothermal power plant in Turkey to verify its effectiveness in a real application. FPS will develop the transient 1D mathematical models for Heat Exchanger and Retention tank, and these models will be included in the D4.4 report, which has the deadline in January 2022.

Selected materials of construction and coatings have been laboratory tested in simulated brine at pH5 in order to support the design of the retention tank, including consideration of anti-scaling coatings. Coatings were selected for their hydrophobicity or 'anti-scaling' properties.

It is duly noted that although this deliverable was originally entitled 'Report on design and building of retention tank', only the design is to be covered herein as the build is covered in WP7.

Objectives Met

With the activities described in this deliverable we will meet the following objectives:

- To transfer technology developments for designing and optimising the scaling reduction system for Zorlu Kızıldere-2 demonstrator, based on the Icelandic experience;
- To extend the knowledge base for design and operation of this and generic similar systems;
- To design a scale reduction system that enables reinjection temperatures down to 50°C, increasing heat recovery;
- To avoid scaling in the reinjection well and to collect silica for further applications
- To investigate materials' and anti-scaling coatings' compatibility with regard to corrosion performance in the simulated geothermal fluid relevant to the retention tank.

1. INTRODUCTION

Geothermal fluids are often strongly enriched with dissolved silica, as these fluids ascend and surface from hot geological formation, they lose their chemical equilibrium. Scaling problems of geothermal fluids put limits on the amount of heat that can be extracted. When geothermal fluids cool down they become supersaturated with respect to secondary minerals and their deposition makes fluid handling very difficult [1]. Uncontrolled silica precipitation on equipment surfaces such as on the reinjection wells, or in the reservoir at the injection site, causes severe damage and operational problems [2].

When geothermal fluids become supersaturated with respect to amorphous silica, the growth of polymers and scale formation are functions of combined chemical and physical processes. Two main types of processes have the tendency to take place: **(1) molecular deposition** of monomeric silica directly onto solid surfaces and **(2) polymerization** of monomeric silica to form silica polymers with homogeneous nucleation and growth of suspended particles. The presence of these two dominant and essentially competing pathways, is shown in Fig. 1 and it has been extensively studied and reported by many authors [1], [3] [4]. The predominance of one process over the other depends on many factors such as water environment, pH-value, ionic strength, temperature, flow velocity, salinity and degree of supersaturation with respect to amorphous silica which is defined as the ratio between silica concentration and equilibrium solubility at the given condition [1].

Many methods have been applied to avoid problems linked with amorphous silica scaling. The common solution is the reinjection of the fluids after the power generation stage into the geothermal wells at temperatures above the temperature of amorphous silica saturation. As a result, the exergy efficiency - particularly the conversion of enthalpy into electrical power - of many geothermal power plants is reduced below 12%: this means poor exploitation of the heat brought to the surface through production wells. This exergy loss can be reduced substantially by taking out more enthalpy from the fluid if the reinjection temperature can be brought down to 50°C (and possibly as far as 20-30°C). In order to reach this injection temperature, different methods have been developed for preventing silica scaling. These methods include retention of water in ponds, use of inhibitors, acidification, silica polymerization and removal of silica from solution ("brine clarification") [5]. The application of coatings has also proven its effectiveness in scaling mitigation. Both organic and inorganic coatings have shown limited fouling when exposed to environments simulating geothermal brine. The deposition of polyphenylenesulfide (PPS) blended with polytetrafluoroethylene (PTFE) onto a carbon steel substrate minimized the deposition of silica when exposed to brine for 7 days [6]. Other examples such as sol-gel TiO2 deposited onto a stainless steel substrate also proved themselves effective against scaling due to a lower surface free energy [7].
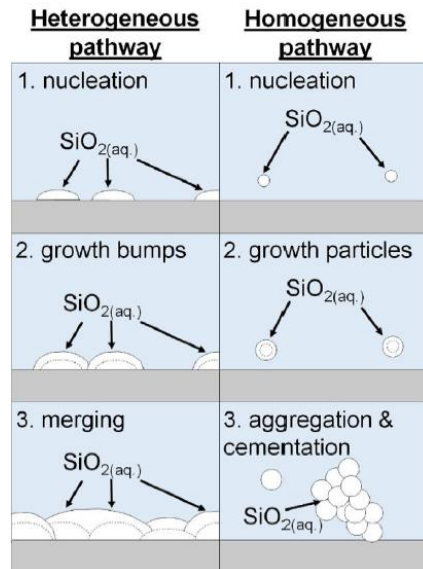
Figure 1: Schematic of the two silica precipitation pathways (SiO2(aq) are silica monomers in solution)

Silica polymerization is used for example to lower silica scaling potential in Nesjavellir and Hellisheiði power plants in Iceland: brines are aged in retention tanks or pipes allowing the monomeric silica in excess of amorphous silica solubility to polymerize [1]. Also Yanagase et al. (1970) reported that, in order to prevent scale adhesion at Otake geothermal plant in Japan, the retaining system can reduce by 10 times the amount of adhesion, using a retention pond where silica is allowed to polymerize [8]. Experience at Olkaria geothermal field in Kenya shows that waste waters do not precipitate silica if stored in a retention pond before disposal into an infiltration pond [5]. It is evident that in some cases storing geothermal waste waters in a retention tank allowing the monomeric silica to form polymers, will reduce the silica scaling potential of the waste waters [9].

In this study we show methods and design of an innovative retention system which will allow to manage silica scaling to reinject brine at 50°C; the system will be demonstrated at Zorlu Kızıldere-2 geothermal power plant in Turkey.

Silica scaling formation and distribution is a key issue in retention system design. The trend of solubility limit of amorphous silica decreases with temperature: when geothermal fluids become supersaturated with respect to amorphous silica the growth of polymers and scale formation are functions of combined chemical and physical processes.
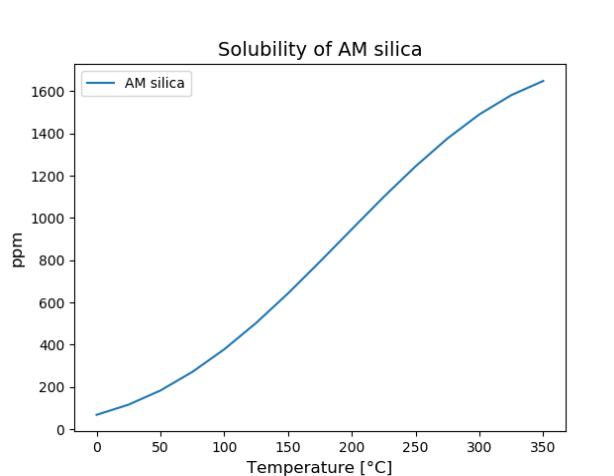
Fig. 2: Solubility of amorphous (AM) silica as a function of temperature

2. PROCESS AND GEOTHERMAL FLUID PARAMETERS

Kizildere was the first geothermal field explored for electricity production in Turkey, starting in the 1960s. Today, the Kizildere geothermal plant operated by Zorlu Energy Inc. comprises of three power plants with a total installed capacity of 260 MWe: the Kizildere-I (15 MWe), Kizildere-II (80 MWe), and Kizildere-III 165 MWe). An evaluation of the Kızıldere site for the implementation of the retention tank was carried out. The brine from Kizildere I is sent to the LP flash of Kizildere II. After the bi-annual meeting held in Kızıldere, it was decided to proceed with the installation of the scaling system after the LP flash unit of Kizildere II.

The Kizildere production fluid is discharged from 1550-2872 m depths with typical reservoir temperatures of ~240-260°C. The geothermal fluids are mainly alkaline bicarbonate with the total dissolved solids (TDS) of ~4500-6000 ppm. The NCG (non-condensable gases dominated by CO_2) concentration in the deep fluid is high ranging from 1.5 to 3 wt%. The Kizildere water is characterized by its high total carbonate concentration and low hydrogen sulphide concentration. The high concentrations of dissolved solids, and especially the high boron and fluoride concentration, make it unsuitable for domestic use or for irrigation. During the steam flashing upon the geothermal fluid utilisation the concentration of dissolved conservative elements and pH increases resulting in formation of microcrystalline $CaCO_3$. $SrCO_3$, $MgCO_3$, SiO_2 and traces of Al, Fe, and K have also been observed [10]. According to the deposit analysis conducted in 2015, there is an increase in Si, Al and Ca content of the deposits from the low pressure separator to the injection wells (Figure 2). About 90% of initial Ca is precipitated in the wells before the fluid reaches the surface.

Scaling has been minimised by controlling the wellhead pressure, assisted by periodic and mechanical removal. Since 2009 inhibitors have also been used to prevent scaling. If inhibitor treatment is not performed $CaCO_3$ and AM silica deposition starts at first production point in the Kizildere-II multi-flash system. At present, there is no major engineering problem with silica precipitation and the reinjection temperature is 104°C. At the Kizildere II where heat exchangers and geothermal brines reach temperatures below 100°C the AM silica scaling potential will be tested as a part of GeoSmart project.

Samples of geothermal water were collected in October 2019 at the point where the reinjection pumps are located and were chemically analyzed at the University of Iceland (UoI). Results of the analysis are reported in Table 1 [11].

Table 1: Chemical composition of re-injection brine at Kizildere II power plant, Turkey

Sample	KZ02 re-injection brine
T°C (sampling)	104
pH/°C	9.77/23
SiO_2	451 ppm
B	24.5 ppm
Na	1335 ppm
K	156 ppm
Ca	4.75 ppm
Mg	0.03 ppm
Fe	0.02 ppm
Al	0.79 ppm
F	27.5 ppm
Cl	111 ppm
CO_2	1053 ppm
SO_4	994 ppm

This subsequent decrease in temperatures may therefore cause AM silica polymerization and silica scaling.

The heat exchanger has been designed during activities in GeoSmart project, matching the speed of heat removal to the thermodynamic speed of silica polymerization such that exergy is released before potential silica scaling can take place. Utilizing high-efficiency rapid heat exchangers that require a much shorter fluid residence

time compared to the silica scaling period, we can control the scale formation and allow the outlet temperature to drop to 50ºC while minimizing silica scale formation.

Silica scaling risks can occur after the heat exchangers, in pumps, pipes and valves of the reinjection wells. For this reason, an optimal scaling-reduction system will be developed to promote the scaling polymerization and harvesting.
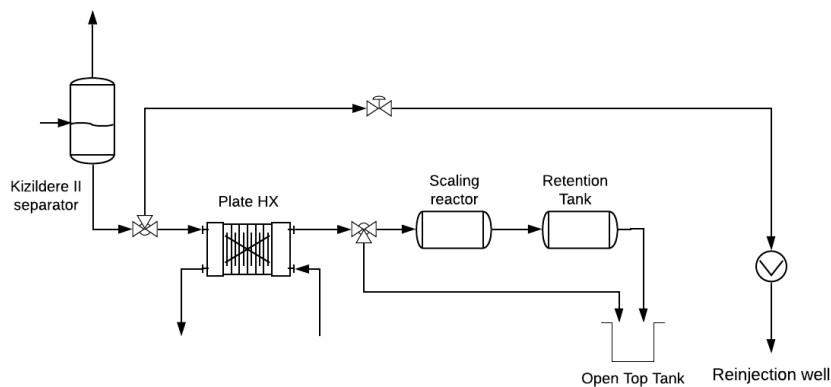
Figure 3: Positioning of the RT system in the geothermal plant

The reinjection water temperature is currently 104°C with a pH of 9.77/23°C. The concentration of aqueous silica in the water is 451 ppm and it is slightly supersaturated with respect to AM silica. The heat-exchanger will recover heat lowering the temperature from 104°C to 50°C with no or very little scaling. This further decrease in temperatures may therefore cause AM silica polymerization and silica scaling in downstream components.

The HX flow rate is set at 50 m³/h; we will take 10% of this flow to be treated into the retention system. The flow of 5m³/h will allow a higher retention time, therefore we will be able to demonstrate the effectiveness and efficiency of the RT system.

Brine properties at Retention System inlet are:

Design Pressure [barg]	Operating Pressure [barg]	Design Temperature [°C]	Operating Temperature [°C]	Flowrate [t/h] [m³/h]	Input RT Silicate conc. [mg/kg]	Input RT pH (23°C)
0.46	0.40	100	50	5.0	451	9.8

3. METHODS

3.1 Equipment design considerations

When geothermal fluids become supersaturated with respect to amorphous silica the growth of polymers and scale formation are functions of combined chemical and physical processes. Two main kinds of processes have the tendency to take place:

1. Molecular deposition of monomeric silica directly onto solid surfaces;
2. Polymerization of monomeric silica to form silica polymers which run with the fluid as suspended particles.

The predominance of one phenomenon over the other depends on various factors, like fluid acidity, velocity (turbulence) and temperature. An accurate study of these processes has been necessary and helpful to find the best design. Molecular deposition involves chemical bonding of dissolved silica directly to solid surfaces like pipe walls, forming hard, dense, difficult to remove and vitreous scale. This mechanism has a slow process, dominant at high flow velocity (turbulence). In reverse, if the solution is in laminar regime, so static or flowing very slowly, silica polymerization inside the solution is the most favoured process [1]: colloids may coagulate and could either precipitate or remain suspended as a semi-solid material and, once silica has polymerized to tetramers, it has less tendency to deposit [18].

pH is one of the parameters which has a stronger effect on polymerization and deposition. In fact, the approach most often used to mitigate silica deposition utilizes the principle of silica solubility as a function of pH, leading to the addition of acids at various points of the system[17].

A mathematical model describing silica scale potential and concentration change of SiO2 with time, referring to Kizildere II geothermal fluid, was carried out during activities of GeoSmart project. Having as inputs temperature, pH and initial concentration, the volume of the scale can be calculated in function of time. The results obtained by this model are significant for the evaluation of the polymerization time. Consequently, they are the basis for the optimal design and choice of the size of the retention system and of the operating parameters which can improve scaling before reinjection wells. In Fig. 4 the trend of silica concentration of Kizildere geothermal fluid with time and pH at 50°C is shown: it has been developed with the model developed by UOI. Keeping pH between 8 and 9 should maximize deposition and polymerization, while maintaining low pH should avoid it.

To test the rate of silica polymerization and scale formation, laboratory experiments were conducted at University of Iceland using solutions with similar chemical composition as the geothermal reinjection water at Kizildere II. It has been concluded that cooling to 70°C results in insignificant SiO2 polymerization and AM silica scale formation. After less than 10 min of reaction time less than 0.5% of the initial SiO2 in solution is expected to have polymerized and after 30 min 0.7-4.7% has been polymerized. The corresponding maximum volume of AM silica formed after 30 min is 0.0014 and 0.0092 cm3 per kg of solution.
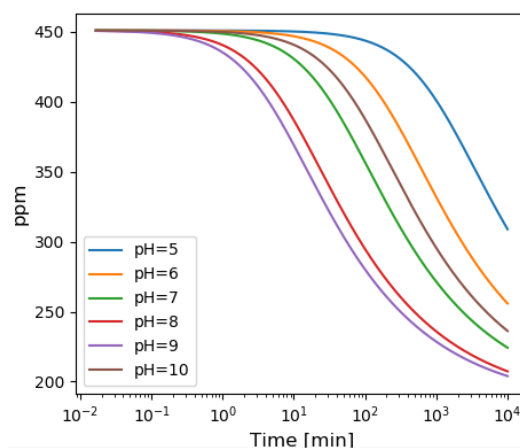
Figure 4 Concentration of SiO2(ppm) in Kizildere fluid at 50°C

At 50°C the input fluid in the retention system has a supersaturation ratio equal to:

$$\frac{SiO_{2\,in}}{SiO_{2\,eq}(50°C)} = \frac{451\ ppm}{183\ ppm} = 2.46$$

Where $SiO_{2\,in}$ is the silica concentration of the mass flow in input and $SiO_{2\,eq}(50°C)$ is the solubility at equilibrium of AM silica at 50°C.

Defining the solubility limit at 50°C as the optimal condition that we aim to reach, the efficiency of the retention system (η_{RS}) can be defined as the ratio of the quantity of SiO2 that has actually polymerized or deposited, to the maximum quantity of SiO2 that should polymerize or deposit to reach the equilibrium value. This parameter will be taken as a reference to evaluate the effectiveness of the RT system (Key Performance Indicator):

$$\eta_{RS} = \frac{SiO_{2\,in} - SiO_{2\,out}}{SiO_{2\,in} - SiO_{2\,eq}(50°C)}$$

where $SiO_{2\,out}$ is the silica concentration of the mass flow in output.

3.2 Coatings and materials
3.2.1 Background

The Geothermal power plant component size and complexity (such as retention tanks, heat exchangers, etc.) as well as rather limited ratio to improve corrosion resistance versus increased costs in most cases exclude solutions based on bulk corrosion resistant alloys (CRAs). Under such circumstances, solutions based on low-cost substrates, such as carbon or low alloy steels with sufficient strength at the operating temperature, in combination with tailored coatings become technically and economically attractive. Anti-fouling coatings have been investigated in the last couple of decades to face the challenges raised by the development of the geothermal powerplants. The use of low-surface energy polyphenylenesulfide (PPS) coatings, first investigated by Sugama et al. [19], has been thoroughly studied for such applications due to its super-hydrophobic nature. PPS was investigated as a matrix in combination with other components such as PTFE, SiC, SiO_2, but also carbon nano-tubes, to provide other properties such as stiffness, corrosion resistance, thermal conductivity among others. Other hydrophobic coatings, such as SiO_2, TiO_2 sol-gel coatings are also relevant alternatives, and showed great corrosion and fouling protection for stainless steel coatings [20]. However, such coatings generally require curing at temperatures up to 500°C, with application such as dip-coating, or line-of-sight techniques such as thermal spraying. For these reasons, commercial paints such as silicon resins, epoxy, ceramic-filled epoxy and others, generally brush applied and cured at room temperature remain valid options as barrier for substrates sensitive to corrosion and fouling [21].

Here, coatings were investigated to protect the surfaces of the retention system which should be kept free of silica scales.

Several coatings systems were studied and the suitable coating system was down-selected based on pre-defined criteria.
- Health and safety compliance
- Corrosion performance
- Mechanical durability
- Wettability
- Ease of application
- Cost
- Market readiness level
- Curing temperature

Based on the above, commercially-available paint systems were selected to be applied to both 304/304L and SA516 Gr60 substrates.

3.2.2 Materials, coatings and weld selection for testing

Two substrates were selected to be tested as part of D4.5 to investigate their corrosion and scaling performance in a simulated geothermal brine consistent with the composition of Kizildere II fluid. The materials that were tested are detailed in Table 2. Duplicate specimens were tested in most cases in order to give reassurance of the test result.

Table 2 Materials and coatings tested

Material/tradename	Reason for selection
304/304L	General-purpose stainless steel grade, widely used where good formability and corrosion resistance are required.
SA516 Grade 60	Typical applications for this steel are reaction and pressure vessels, as well as pipework
Belzona 1341	Two-part epoxy coating designed to improve efficiency of fluid handling equipment while protecting them from erosion and corrosion. Developed as hydrophobic to repel process fluids and reduce turbulent flow.
Sakaphen Sakatonit Extra AR	Cold cured amine Epoxy system – hydrophobic, mechanically durable in all types of water and acidic to strongly alkaline media

Multi-pass butt welds were made in 304L stainless steel and the SA516 Grade 60 steel using filler wire and the TIG welding process. The welds are summarized in Table 3. Full details are given in the WPS presented in Appendix A. Figure 5 shows photograph of two of the welded plates prior to cutting.

Table 3 Weld details

Material/tradename	Filler metal	Welding preparation
304/304L	ER308L	Double-V
SA516 Grade 60	ER70S-2	Double-V
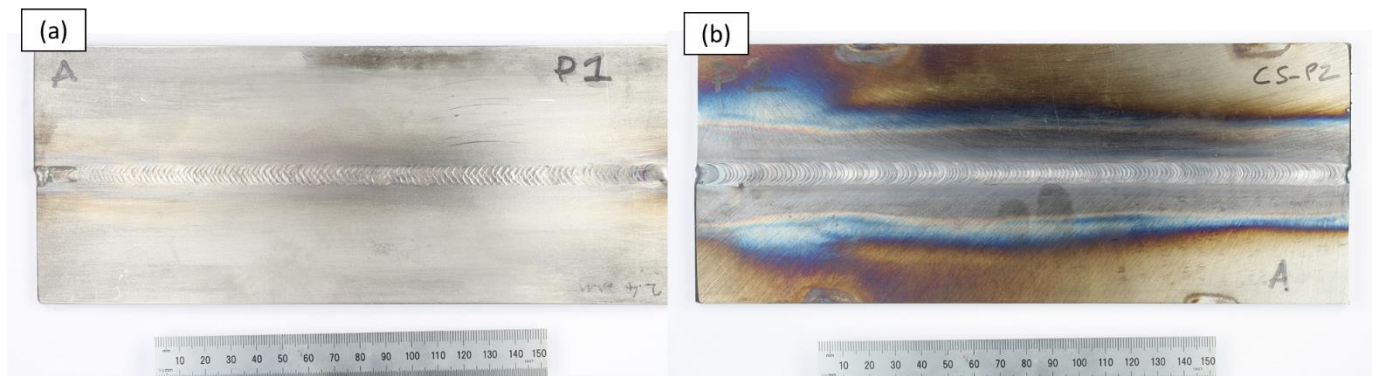
Figure 5 304/304L (a) and SA516 Gr60 (b) welded plates prior to sample preparation

3.2.3 Sample preparation

3.2.3.1 Pitting and general corrosion

In order to investigate the potential corrosion behavior of the selected materials and coatings in the simulated brine environment, 50x20x5 mm coupons were prepared. The coupons were drilled according to the drawing shown in Figure 6(a), to accommodate the sample stand (top hole). Electrical isolation between bolts and specimens was ensured. Both selected coatings were applied on larger substrates (40x40x5 mm) to facilitate application and sealing.
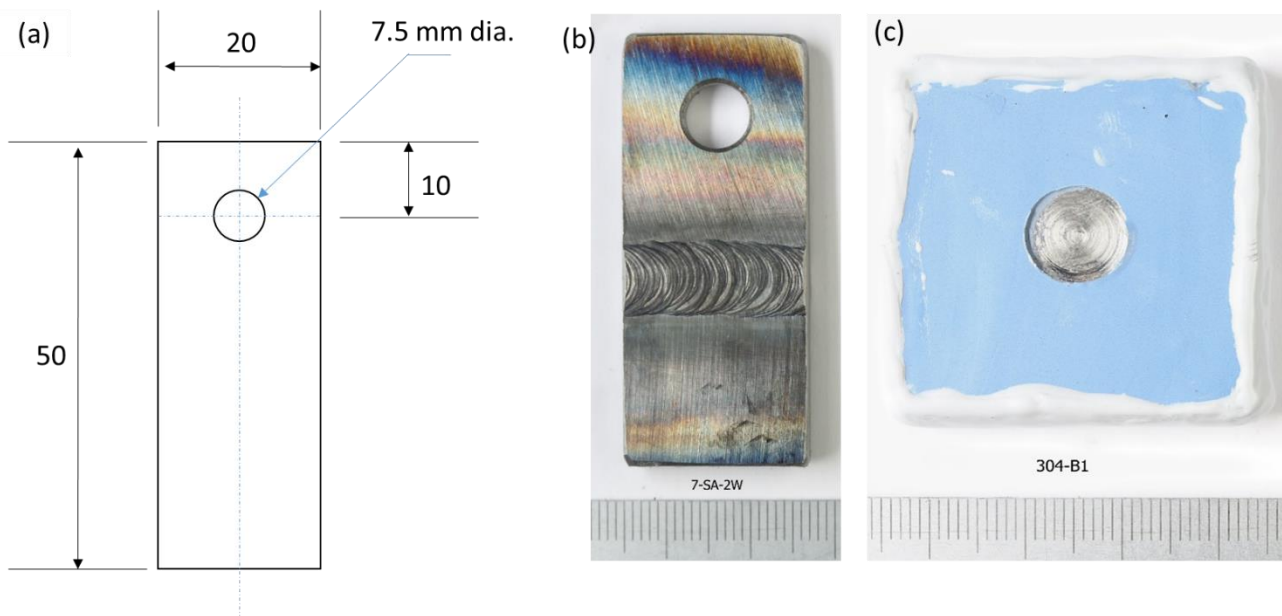
Figure 6 Drawing of parent material corrosion specimens and associated dimensions (a), welded specimens (b) and photograph of a coated specimen with a holiday (c).

3.2.3.2 Stress-corrosion cracking specimens

To evaluate the potential stress corrosion cracking in the materials considered for the heat exchangers, U-bend specimens were also prepared in 304/304L stainless steel. Following the ASTM G30-97 standard, a rectangular strip was bent at 180° around a predetermined radius and held in place using a Ti grade 2 bolt. The samples were insulated from the bolts and nuts by using ceramic washers and by ensuring the bolt would be secured at

the centre of the clearance hole. Figure 7 shows the design of the U-bends and labels the critical dimensions.
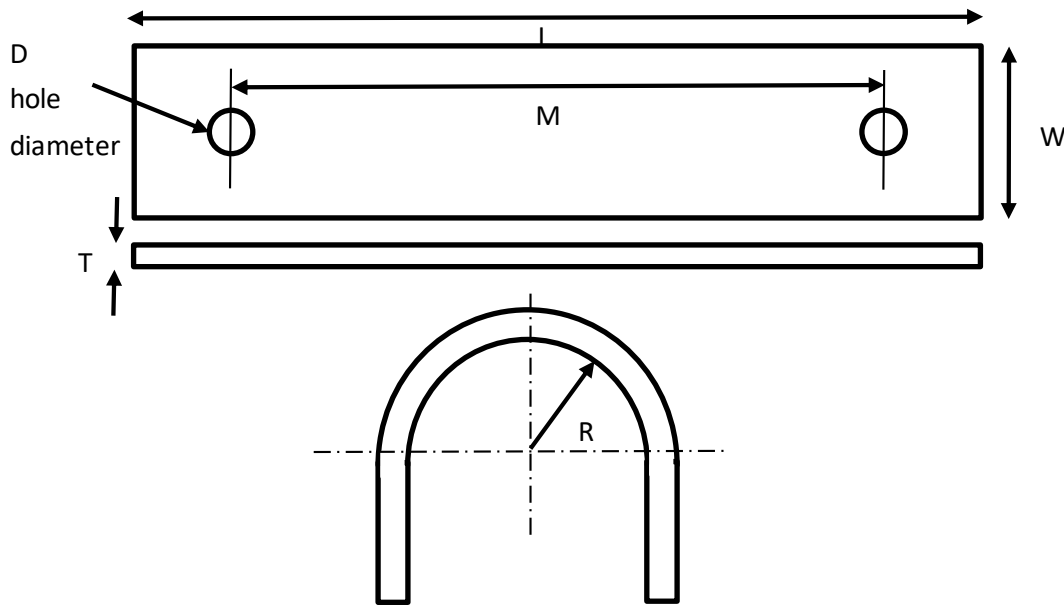
Figure 7 U-bend dimensions and design

In this work, dimensions were selected as per the following:

Table 4 Dimensions of U-bend specimens

M	150 mm
L	180 mm
T	5 mm
W	20 mm
D	9 mm
R	30 mm

The outer tensile face of each individual U-bend strip was ground to Ra<0.8 μm prior to bending. Roughness was measured using optical profilometry.

3.2.3.3   Coated specimens

40x40x5mm specimens were coated using both selected paints. Substrates were grit blasted prior to coating application. Details of the paint application are given below:

Belzona 1341

A two-coat system at an average of 250 μm per coat was applied on both SA516 and 304/304L substrates. Cured at room temperature,

Sakaphen Sakatonit Extra AR

A 3-coat system was applied, with an approximate thickness of 150 µm per pass. The two components (material and hardener) were mixed to the appropriate ratio (77/23). 8 hours were left between each pass. Brush application was used to

3.2.4 Corrosion testing

3.2.5 Environment and experimental design

3.2.5.1 Brine recipe

The chemistry used in the simulated environment was based on the field conditions that were measured at the Kizildere II geothermal power plant after the low pressure separator, as well as the conditions used as part of D4.2 (Report on formulation of inhibitor against silica scaling, submitted M12), see Table 5. The solution composition for the tests was chosen to include the elements that would be corrosive to the metals and alloys (chloride), control the pH (DIC), and/or would be involved in the scaling (SiO_2, Ca, Mg).

Tests were deaerated and carried out under 99.998% Ar to simulate the environment after the separator.

Testing temperatures were based on the minimum and maximum operating and design temperatures of the heat exchanger. The maxima were targeted because corrosion processes tend to be accelerated at higher temperatures. In a similar fashion, a lower pH of a more acidic media can accelerate these processes. The system is partially exposed to brine at pH 8 and partially exposed at pH5, so, pH 5 was selected for the tests as being the more aggressive condition.

In order to make the solution, the SiO_2 was dissolved into in 0.1M NaOH before being mixed with a solution of $NaHCO_3/Na_2CO_3$. The chloride was then added as $CaCl_2.2H_2O$ and $MgCl_2.6H_2O$. HCl (0.1M) was then added to reach the required pH5.

Table 5 Basis of brine composition for corrosion tests. Items in Bold were employed in the corrosion testing.

Constituent	Brine, mg/l
pH/23°C	**5**
SiO$_2$	**451**
B	24.5
Na	1335
K	156
Ca	**4.75**
Mg	**0.03**
Fe	0.02
Al	0.79
F	27.5

Cl	111
CO_2 (=DIC)	1053
SO_4	944

3.2.5.2   Tests 1 and 2 – long-term exposure in simulated geothermal brine

Initial tests were designed to evaluate the ability of the selected material to withstand extensive immersion in geothermal brine at elevated temperature. Both Tests 1 and 2 were thus conducted in relatively large autoclaves, at 104°C. Both vessels were purged using 99.998% Ar, and tests were conducted at a pressure of 5 barg. Glass liners were used in the autoclaves. The test duration was 29 days.

Table 6 Sample labelling for exposure tests

Tests	Duration	Substrate Tests	Pitting corrosion (20x50x5mm)				U-bends		Coated			
			Bare		Welds				Belzona 1593		Sakaphen	
Test 1 - 104 °C - static - pH 5	29 days	304/304L	7-304-1	7-304-2	7-304-1W	7-304-2W	1-304-U1	1-304-U2	304-B1	304-B2	304-S1	304-S2
Test 2 - 104 °C - static - pH 5	29 days	SA 160 Gr60	7-SA-1	7-SA-2	7-SA-1W	7-SA-2W	--	--	SA-B1	SA-B2	SA-S1	SA-S2

Table 6 indicates the various samples and materials used for the autoclave tests in simulated geothermal brine. Each setup is detailed further below.

Test details

Test 1 was performed in a larger autoclave. The sample stand was designed using 2 metallic rods covered in heat shrink, where 6 samples (4 welds and 2 U-bends) were installed. The 4 coated samples, non-drilled, were however placed in Hastelloy baskets. Two baskets, each containing two samples, were placed in the autoclave below the sample stand. The dimensions of each basket were the following: 150 mm length, 60 mm maximum width and 850 mm depth. Figure 8 shows a photograph of one of the Hastelloy baskets used in Test 1.

Test 2 was performed in a smaller autoclave, and samples were thus placed onto a narrower sample tree. Similar to test 1, two Hastelloy baskets were placed in the autoclave, each containing two coated samples.
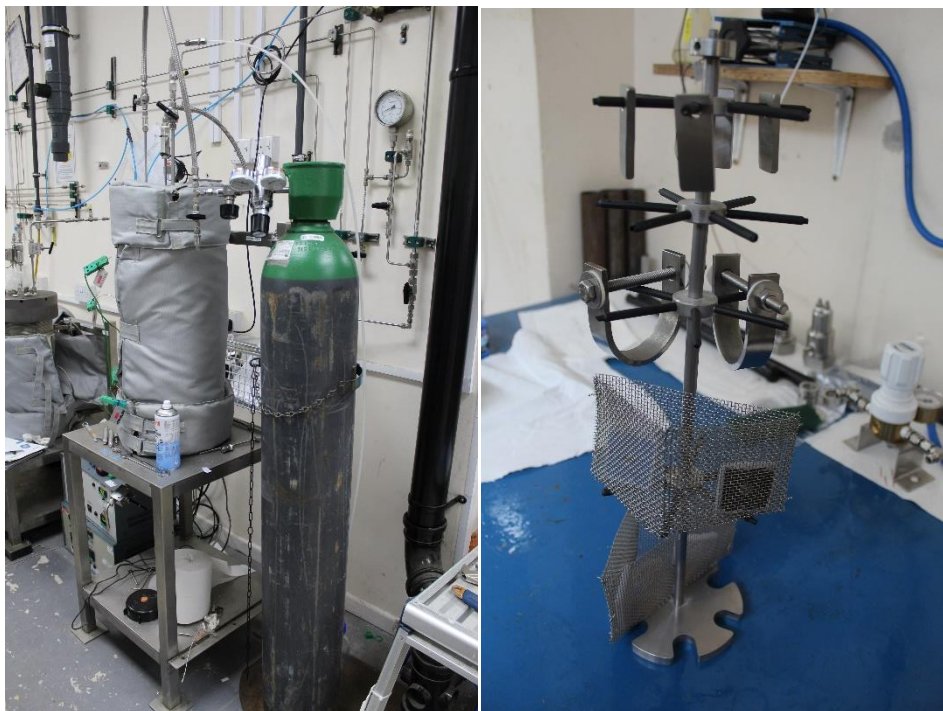
Figure 8 Picture of the autoclave during testing (left) and of the sample holder prior to insertion in the autoclave (right)

For Test 2, the sample stand was designed using 2 metallic rods covered in heat shrink, where 8 samples (2 parent material coupons, 2 welds, 4 coated samples) were installed.

Figure 9 Photograph of the autoclave containing the samples tested at 50°C

3.2.6 Post-test characterisation

3.2.6.1 Visual examination

Specimens were visually examined before and after testing. Photographs were taken to record observations.

3.2.6.2 Mass loss

The corrosion specimens and U-bend specimens (with bolts) were weighed before and after testing in order to evaluate the extent of any corrosion. Specimens were not cleaned before weighing after test in order to evaluate the extent of scaling.

3.2.6.3 Optical profilometry

The topography of the coated samples before and after exposure was characterized using the Alicona InfiniteFocusSL (Bruker, Austria). Through non-contact 3D optical measurement, a surface of approximately 5x10 mm was characterized on each selected coupon, using a 20x objective corresponding to a vertical resolution of 100 nm.

3.2.6.4 Non-destructive testing

Dye penetrant testing (DPI) was carried out on the tensile face of the U-bend samples in order to look for cracking. Photographs were taken to record observations.

3.2.6.5 Scanning electron microscopy (SEM)

SEM and EDX (energy dispersive X-ray spectroscopy) were used to examine one of each of the duplicates of long-term corrosion specimens after testing. The most corroded/scaled specimens were selected visually for this examination.

4. RESULTS AND DISCUSSION

4.1 General layout

The scheme of the retention system we designed is shown in the following image; it has two effects on geothermal fluid, which follow respectively the two processes previously described in Methods:

1. Firstly, in the scaling reactor, molecular deposition on surfaces is promoted by high pH and Turbulence; here we will collect the silica deposits for further applications.
2. Secondly, in the retention tank, silica polymers formation is promoted by lowering the pH to 5 and in laminar flow, reducing the tendency to deposit in the reinjection well.
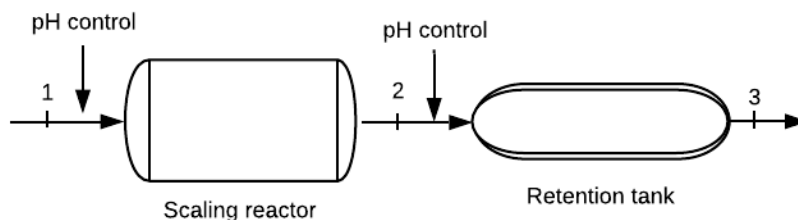
Figure 10: Layout of the RT system

In the initial part of the retention system, where the concentration of the fluid is well above the solubility limit and, consequently, the scaling potential is high, silica deposition is maximised. Once the monomeric silica concentration has become lower, also the probability of scale deposits decreases: after the scaling reactor, the geothermal fluid enters in an actual retention tank, where remaining silica monomers can polymerize. In this way, further reducing silica scaling with the dilution of the fluid with water and with the addition of inhibitors, the monomeric silica concentration is minimized before reinjection, reducing scaling problems in well pipes.

To maximise the probability of deposits, the **scaling reactor** has been designed with: (a) a suitable geometry in order to increase contact area between flow particles and surfaces; (b) an appropriate mechanism for

promoting turbulence and the number of impacts between particles and surfaces; (c) pH control to reach 8/9 inside. To control the flow pH additional substances are mixed with the geothermal fluid in point 1.

Once the majority of silica in the flow has been collected, the low silica-concentration flow rate enters an actual **retention tank**. To increase monomeric silica polymerization, it has been designed with: (a) a suitable geometry in order to let the brine stay in laminar flow avoiding contact with surfaces; (b) pH control to lower it.

4.2 Specific design

A drawing of the **scaling reactor** design is shown in the annexes drawings. It is a 10 m^3 square tank with two removable "doors/drawers": 10 panels cross the tank transversely (5 per door) and each one of them has 4 smaller panels placed in the longitudinal direction. All these plates (a) create an obligatory path for the fluid inside the reactor and (b) are removable with the "doors/drawers". In this way (a) turbulence inside the reactor is made by the path itself which increases the flow velocity and the contact area between plates and fluid and (b) panels where scales are maximised can be easily cleaned and silica collected.

The "doors/drawers" have been designed to make the opening phase as easy as possible. They will run on inside rails and 2 additional "outer" rails will be supplied to facilitate the operating.

At the inlet we will control pH with addition of substances. The desired pH inside this component is around 8 as, from the mathematical model developed in D4.1, it should be the best value to maximise deposition.

The last component is a "classic" cylindrical 10 m^3 **retention tank**, where the fluid slowly flows in laminar flow and silica polymers can develop and run with the fluid without scaling on surfaces.

At the inlet we will control again pH with addition of substances. The desired pH inside this component is around 5 as, from the mathematical model developed in D4.1, it should be the best value to avoid deposition.

For the **material** selection the scaling reactor, where we expect high deposits, will be made in Stainless Steel AISI 304L, while the retention tank, where scaling should not occur, will be made in carbon steel SA516 Gr. 70. All components will be insulated to avoid further decrease of flow temperature with Rockwool of 50 mm thickness, density 120 kg/m3 (finishing with aluminium sheet 6/10mm).

Coating would be necessary for the inner surface of the retention tank regarding that commercial acids would be used to reduce pH value to 5. Coating with epoxy vinyl ester FRP material is recommended for better operating conditions to avoid corrosion in the retention tank.

Turbulence models and simulation

A CFD analysis has been carried out to define the best geometry inside the scaling reactor; the turbulence has been maximized with low pressure drops.
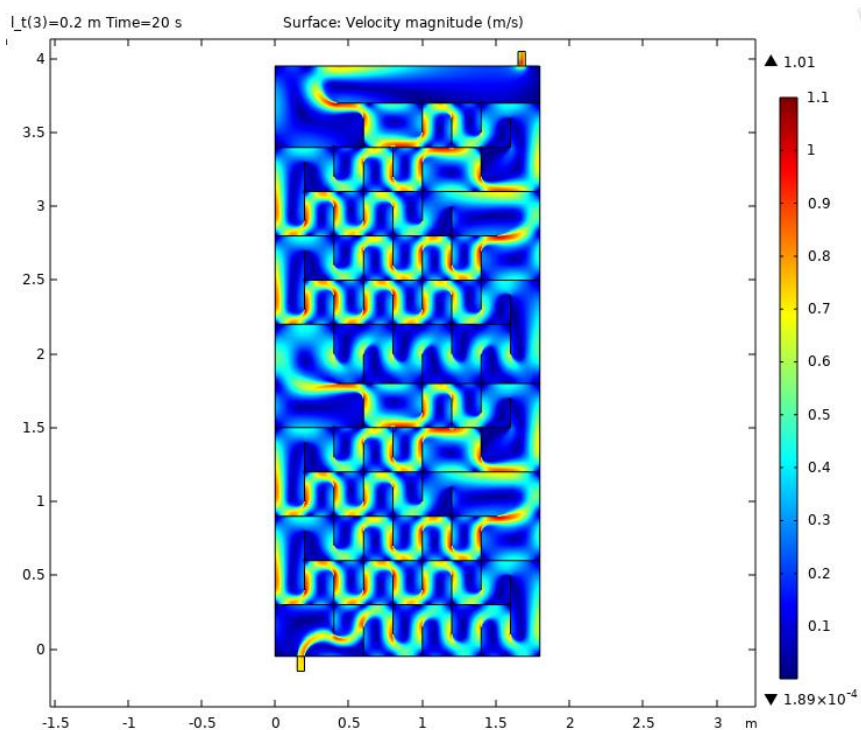
Figure 11: Scaling Reactor CFD model (by COMSOL® software)

FEM

As the scaling reactor will be built as a rectangular tank a FEM has been carried out to identify the positioning and dimensioning of the stiffeners.
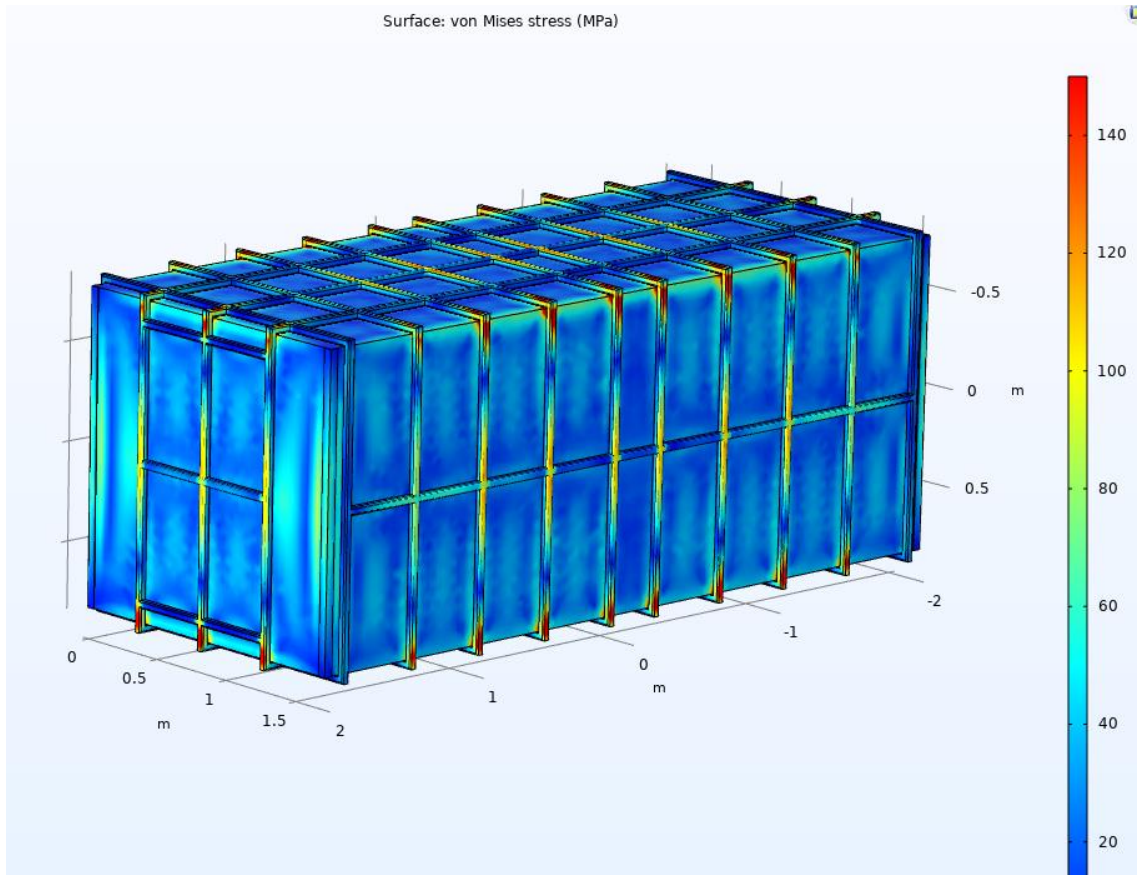
Figure 12: Scaling Reactor Von Mises Stress analysis (by COMSOL® software)

4.3 Silica Extraction System

The shape of the scaling reactor is mostly due to the extraction system for silica removal: it was designed to extract the inner plates were silica deposits will occur. The opening system of the M1/M2 doors of Scaling Reactor was designed with no. 8 wheels which, sliding on two internal tracks and two external tracks to the vessel, it will allow easy extraction and an equally easy closing phase.

The weight or size of each door, including the internals fixed to it, will not be a problem during the opening and closing phase because the wheels used are amply sized for the weight to be supported.

At this stage, we cannot assess whether post-process wheel fouling can reduce the sliding capacity of the wheels and consequently more force will be required to be exerted to pull the door. If this event occurs, we believe that the adoption of an electric winch hooked to the door handles can solve this problem.

Below are reported the steps of opening door procedure:

Step 1: the doors are closed and the process has been interrupted. Verify that the operating temperature has decrease to ambient temperature before thermal insulation removal. Verify that the operating pressure is at ambient pressure before unscrew n.54 nuts on each flange for doors opening.

Step 2: open at least 250mm the door by pulling it using the front handles; remove the sealing gasket and check it. Assemble the first two front sliding wheels.

Step 3: open additional 110mm the door by pulling it using the front handles. Assemble rear two pair sliding wheels.

Step 4: pull internal units until the end of the sliding rail and proceed with the cleaning and disassembly of the removable internal panels. Repeat operations in reverse way to reassemble the units. Replace gasket if necessary.

1.ST STEP OPENING DOOR PROCEDURE

3.RD STEP OPENING DOOR PROCEDURE

4.TH STEP OPENING DOOR PROCEDURE
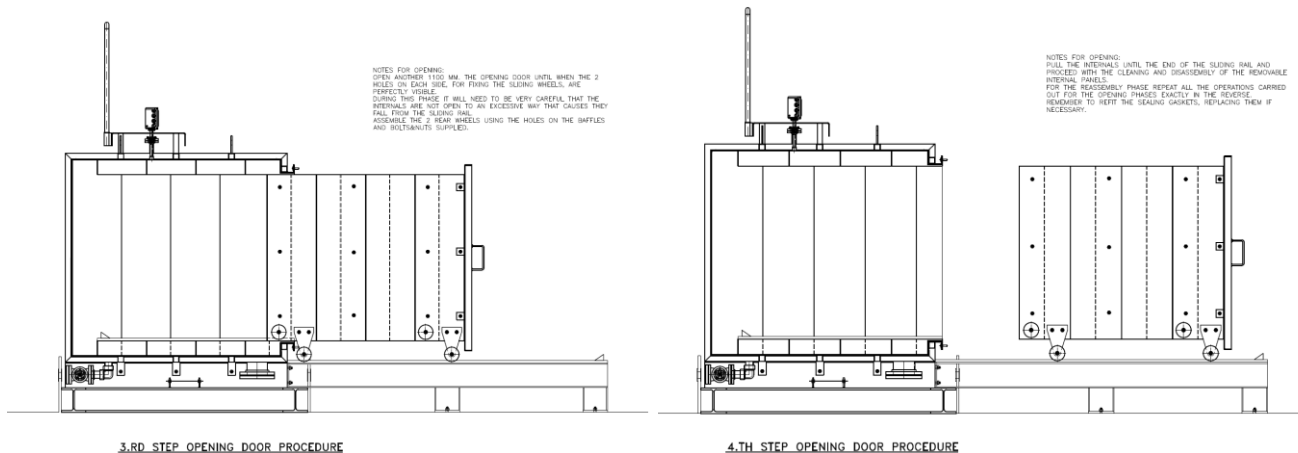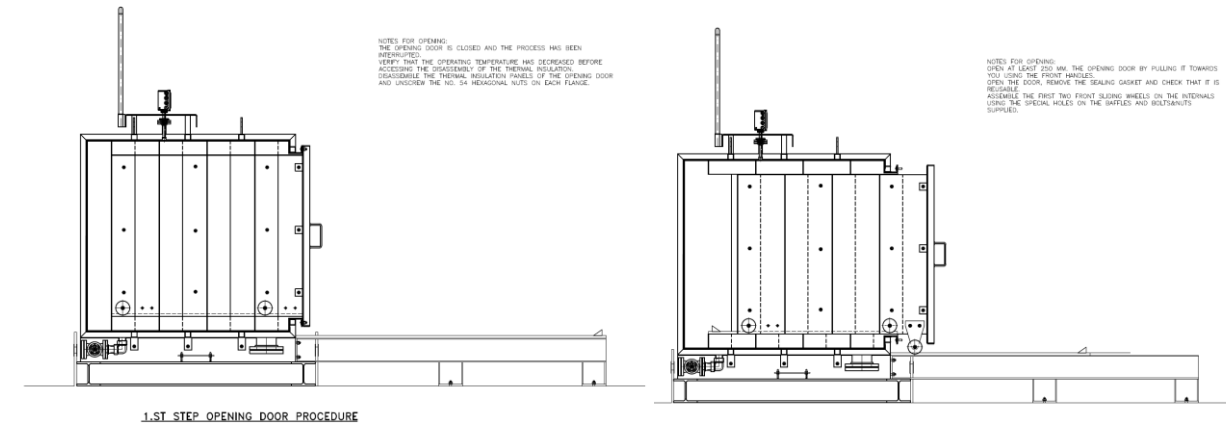
4.4 Instrumentation and control

For the **instrumentation and control**, the following sensors/sample ports will be installed, as shown in the P&ID attached. Following the streamline:

- Upstream of the scaling reactor:
  - 1 sampling port to collect fluid;
  - 1 flowmeter;
  - 1 pressure sensor;
  - 1 temperature sensor;
  - 1 valve for acid inlet to control pH inside the reactor;
- In the scaling reactor:
  - 2 pH sensors, one at the inlet and one at the outlet of the component;

- - o 1 temperature indicator;
    - o 1 pressure indicator;
- Downstream from the scaling reactor and upstream of the retention tank:
    - o 1 sampling port to collect fluid;
    - o 1 temperature sensor;
    - o 1 pressure sensor;
    - o 1 valve for acid inlet to control pH inside the tank;
- In the retention tank;
    - o 2 pH sensors, one at the inlet and one at the outlet of the component;
    - o 1 temperature indicator;
    - o 1 pressure indicator;
- Downstream from the retention tank:
    - o 1 sampling port to collect fluid;
    - o 1 temperature sensor.

All the sensors will be connected to a data logger for data acquisition.
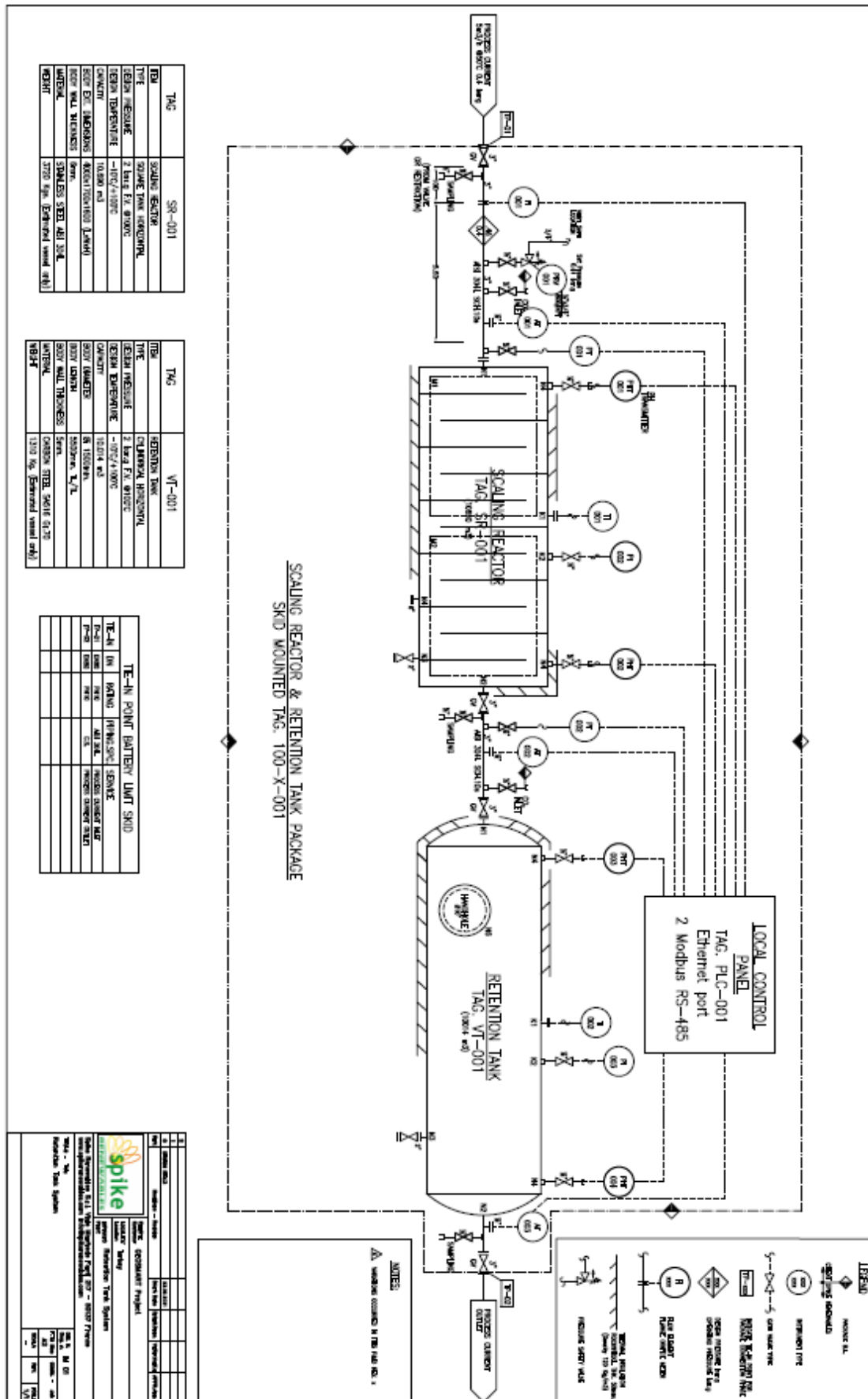
Figure 13: P&ID of the system

4.5 Economics and Environmental Impact

The development of a system for enhancing silica capture and silica scaling prevention has benefits in terms of economic investment and for reducing greenhouse gases (GHG) emissions. By resolving silica scaling issues in the reinjection wells, there is the possibility to couple the geothermal plant with an additional low-temperature Organic Rankine Cycle system (ORC) for electricity production as well as the recovery of waste thermal energy in order to use it in the local District Heating or for industrial applications. An additional advantage is the sale of silica which is a material used for many applications, such as in the construction industry (production of concrete and insulation panels), glass industry and other minor sectors (food, cosmetic, and pharmaceutical).

An economic and environmental analysis for the retention system has been carried out for Kizildere 2 site, considering the total mass flow capacity of the plant and not only the quantity that will be tested inside the GeoSmart system. In this way we aim to demonstrate the feasibility and possibility of the retention system to be scaled up. The geothermal fluid has an available temperature at 104°C. Considering an injection temperature at 50°C and a mass flow rate of 1700 tons per hour, it is possible to recover about 936 GWh of thermal energy. The monthly averaged thermal demand of the existing District Heating of Kizildere is shown in Table 7; consequently, a 25 MW system is sufficient to satisfy the thermal demand in coldest months of the year.

Table 7: District Heating demand in Kizildere

Month	Heat Demand (MWh)	Thermal power (MW)
January	18449	25
February	13450	20
March	14115	19
April	9490	13
May	0	0
June	0	0
July	0	0
August	0	0
September	0	0
October	0	0
November	4439	6
December	7114	10

With the retention time previously defined, we are able to obtain 1799 tons of silica per year which, considering a market price of 50€/ton, has a global revenue of about 90 thousands of euros per year. The retention tank system costs are estimated considering as construction materials Stainless 316L or DUPLEX. These materials have fluid operative conditions and corrosion resistance suitable for this application.

The results underline that the installation of the system in Kizildere site is expected to be profitable. The Pay Back Period will be at around 7 years and the net present value (NPV) could reach more than 60 million of euros

(about double the initial invested capital). The solution proposed has benefits also in terms decrease of GHG emissions because the energy (thermal and electrical) is produced by waste heat, otherwise lost in the reinjection process. Moreover, the reduction of environmental impact is estimated in tons of equivalent oil avoided, which reaches almost 755 thousand of TOE per year in comparison with a district heating which uses natural gas as heat source. These savings give also the possibility to have access to national incentives.

4.6 Chemical compatibility results
4.6.1 Corrosion

Table 8 Results of corrosion tests

Sample label	Weight loss (-) /gain (+) after test, g	Weight loss (-) /gain (+) after cleaning after test, g	Corrosion rate , µm/year
7-304-1	+0.0044	+0.0012	NA
7-304-2	+0.0035	+0.0005	NA
7-304-1W	+0.0049	+0.0013	NA
7-304-2W	+0.0046	+0.0010	NA
7-SA-1	+0.0662	-0.0910	60
7-SA-2	+0.0581	-0.0829	57
7-SA-1W	+0.0492	-0.1255	72
7-SA-2W	+0.0578	-0.1367	78

Table 8 shows the weight difference measurements which mostly showed weight gain. This correlated with the visual observations of scaling of the samples in both tests. The results of the further post-test evaluations are shown in Appendix B. These confirmed the presence of silica scale on all of the specimens examined, but also the presence of Ca-rich and Mg-rich areas. Orange corrosion products were visible on the steel samples. The weld metal and heat-affected zone (HAZ) appeared to have suffered less corrosion than the parent metal on the steel.

The visual examination showed different surface state of the stainless and the carbon steel, with a large amount of corrosion products on the surface of the latter. EDX analysis showed similar results across most characterized samples: the presence of Si scaling was consistent across all analyzed samples, with limited $CaCO_3$ scaling.

Corrosion rates were measured following the cleaning, conducted following ASTM-G1 based on the weight change and the surface area of the sample. Although 304/304L samples did not show any weight loss following cleaning, corrosion rates between 57 and 78 µm/year were measured for both weld and parent material SA516 coupons. Consistency was seen across the characterised samples, suggesting reproducibility in the conducted experiments.

4.6.2 U-bends

White scale was observed on the surface of both U-bends after test. There were one or two dark spots on the stressed end of each of the samples, consistent with localized corrosion products. The DPI results of the U-bend testing confirmed that no cracking was observed. Weight change measurements – with the bolts attached – showed slight weight gain, as can be seen in Table 9.

Table 9 Results of U-bend tests

Sample label	Weight gain, g	Cracks	Pits
1-304-U1	0.0192	None	3
1-304-U2	0.0093	None	2

The results of the post-test evaluations are shown in Appendix C. Optical profilometry was conducted on a pit on each U-bend, and 1.8x1.8 mm wide areas were scanned to evaluate the pits, including a profile taken across a pit on sample 1-304-U2 to evaluate its depth. The pit characterized on sample 1-304-U1 showed no depth, suggesting that most features scanned on the surface corresponded to corrosion products. On the other hand, the pit scanned on sample 1-304-U2 showed 4-5 µm of depth.

4.6.3 Coated samples characterisation

Optical profilometry

Two selected coatings were applied to both SA 516 and 304/304L substrates. A defect was simulated by drilling a hole through the coating up to the substrate. Before and after exposure to the geothermal brine, they were characterised using optical profilometry. As the samples were exposed to the aggressive environment, differences in surface profile of the drilled area can be evaluated by non-contact profilometry. Figure 14 shows that approximately 700µm-deep defects were drilled through the coating and up to the substrate. No difference can be seen on the surface profile of the 304/304L samples, however a slight difference in profile can be seen for the carbon steel sample that can be attributed to corrosion products as it can be seen in Appendix B.
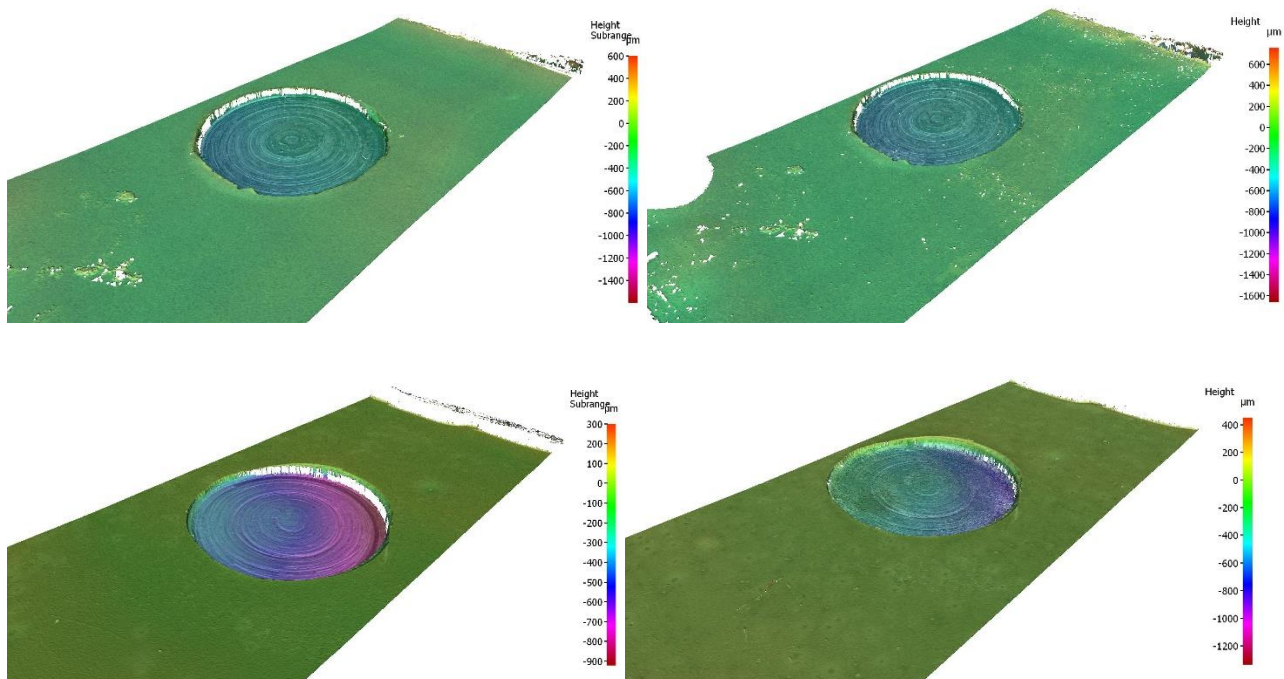
A profile was taken across the drilled material in samples 304-B1, and the corresponding profile was plotted below. Drilled with a diameter of 10 mm, it reached a depth of 600 µm. The drilling procedure caused the applied coating to be lifted on the edges, as highlighted in Figure 14.

Surface profile of Sample 304-B1
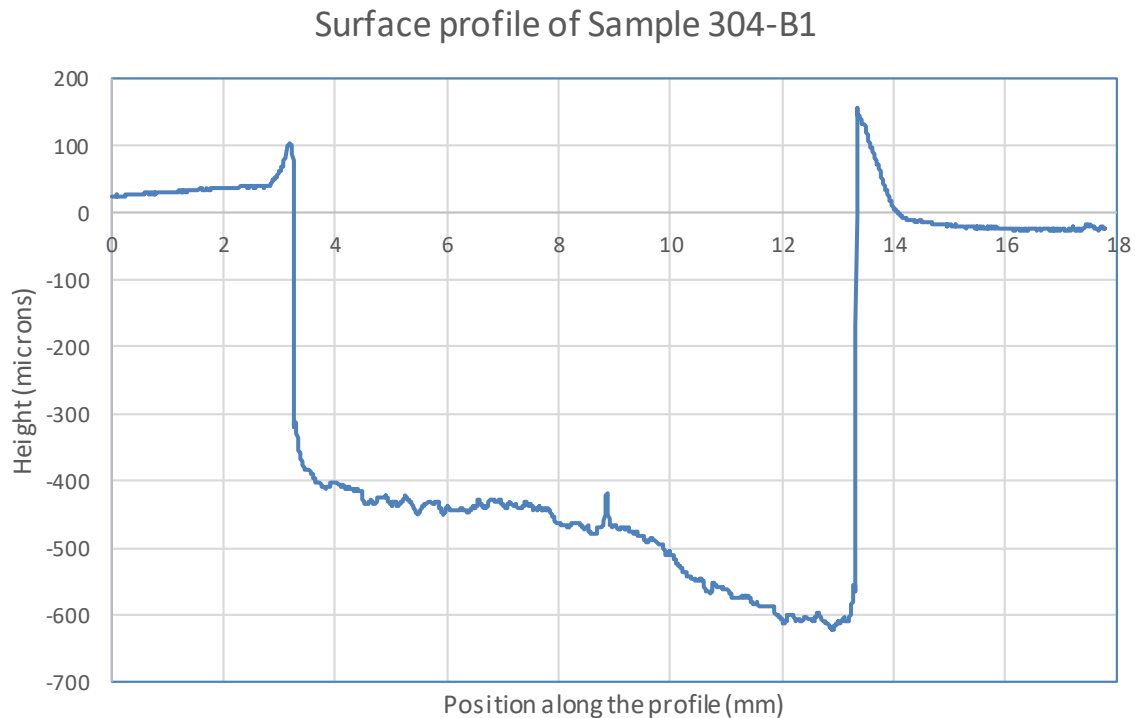
Figure 14 Profile taken across the drilled defect showing its depth and the general surface profile.

Bond strength

Portable adhesion testing was conducted on coated samples to evaluate the adhesion of the selected paint to the substrates. The results of the tests are presented in Table 10. All coatings failed cohesively, meaning that the failure occurred between one of two layers of paint; the coatings being a two-layer system. The load to failure values are expected to be more than adequate for this application, which required 4MPa as a KPI [23]. While reported and measured values are lower compared to the values quoted by the manufacturer, the manual application can be responsible for variations in mechanical performance.

Table 10 Bond strength measurements following PAT on coated specimens

Coating	Substrate	Load to failure (MPa)	Failure mode
Belzona 1341	304/304L	25.6	Cohesive
		23.4	Cohesive
		24.6	Cohesive
	SA516 Gr60	24.4	Cohesive
		24.3	Cohesive

		25.6	Cohesive
Sakaphen AR	304/304L	13.5	Cohesive
		16.4	Cohesive
		12.6	Cohesive
	SA516 Gr60	15.4	Cohesive
		13.5	Cohesive
		13.6	Cohesive

Scanning electron microscopy on sections

304/304L samples

Figure 5 shows the cross-section of the 304/304L samples with the two different coatings. The sample coated with Belzona appears to have consistent thickness, and bonds with the substrates even in the vicinity of the drilled area. On the other hand, the sample coated with Sakaphen appears to have debonded following drilling. On both samples, no corrosion product or scaling can be seen on either the coating surface or the drilled area.
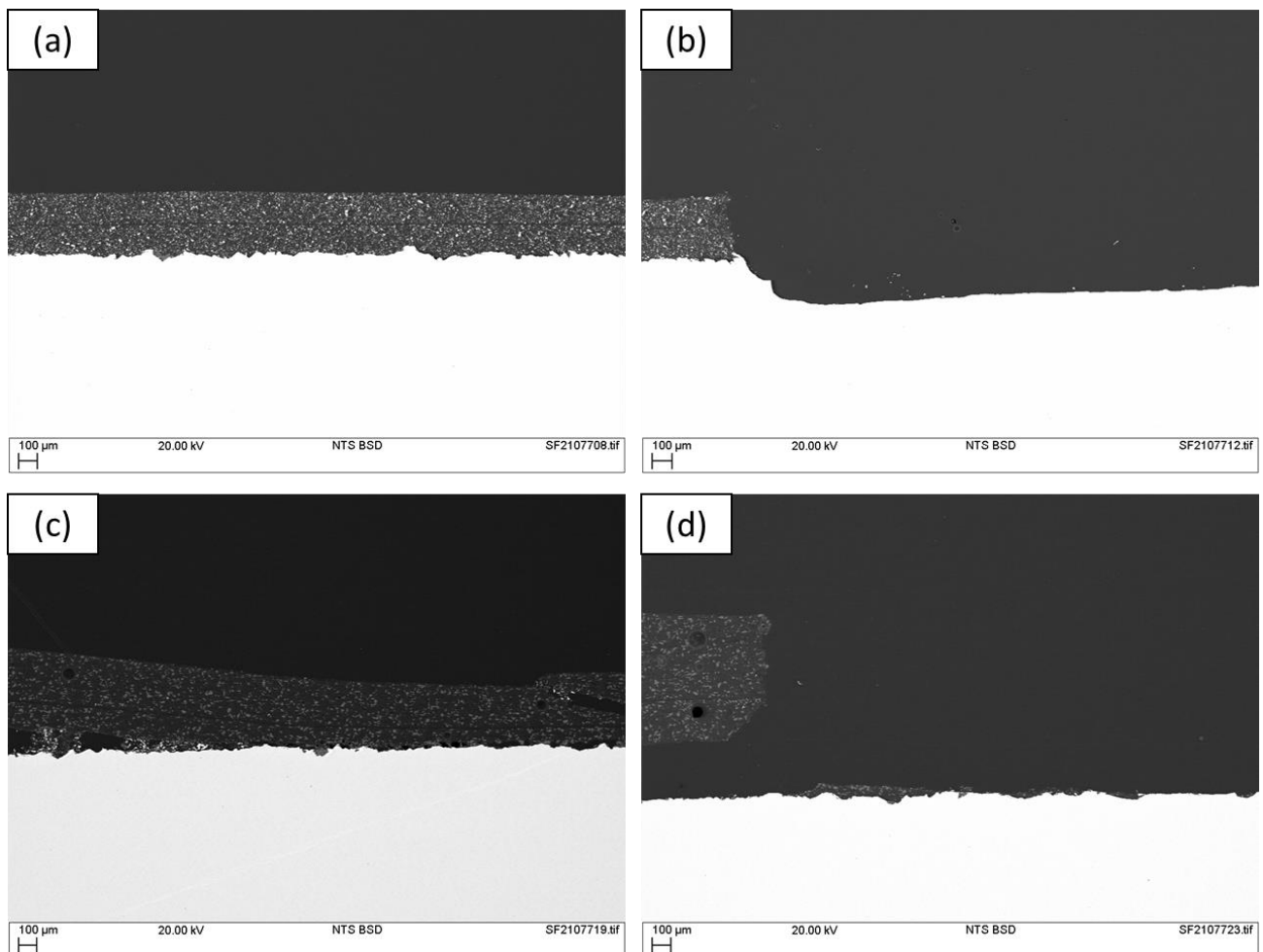
Figure 15 Cross-section of samples 304-B1 (a,b) and 304-S1 (c,d), showing the coating thickness as well as the defect area.

Figure 1626Figure shows the cross-section of the carbon steel samples with the two different coatings. Both samples are showing good bonding with the substrates even in the vicinity of the drilled area. On both samples, corrosion products can be seen on the surface of the exposed substrate, however nothing can be seen over the coated area. Both Figure 38 and Figure 49 correspond to the SEM and EDX analysis of the corrosion products observed on the surface of samples SA-B1 and SA-S1 respectively. The EDX analysis, similar in both cases, suggests that the features observed in the defect area correspond to a mixture of Silica scaling and Fe corrosion products.
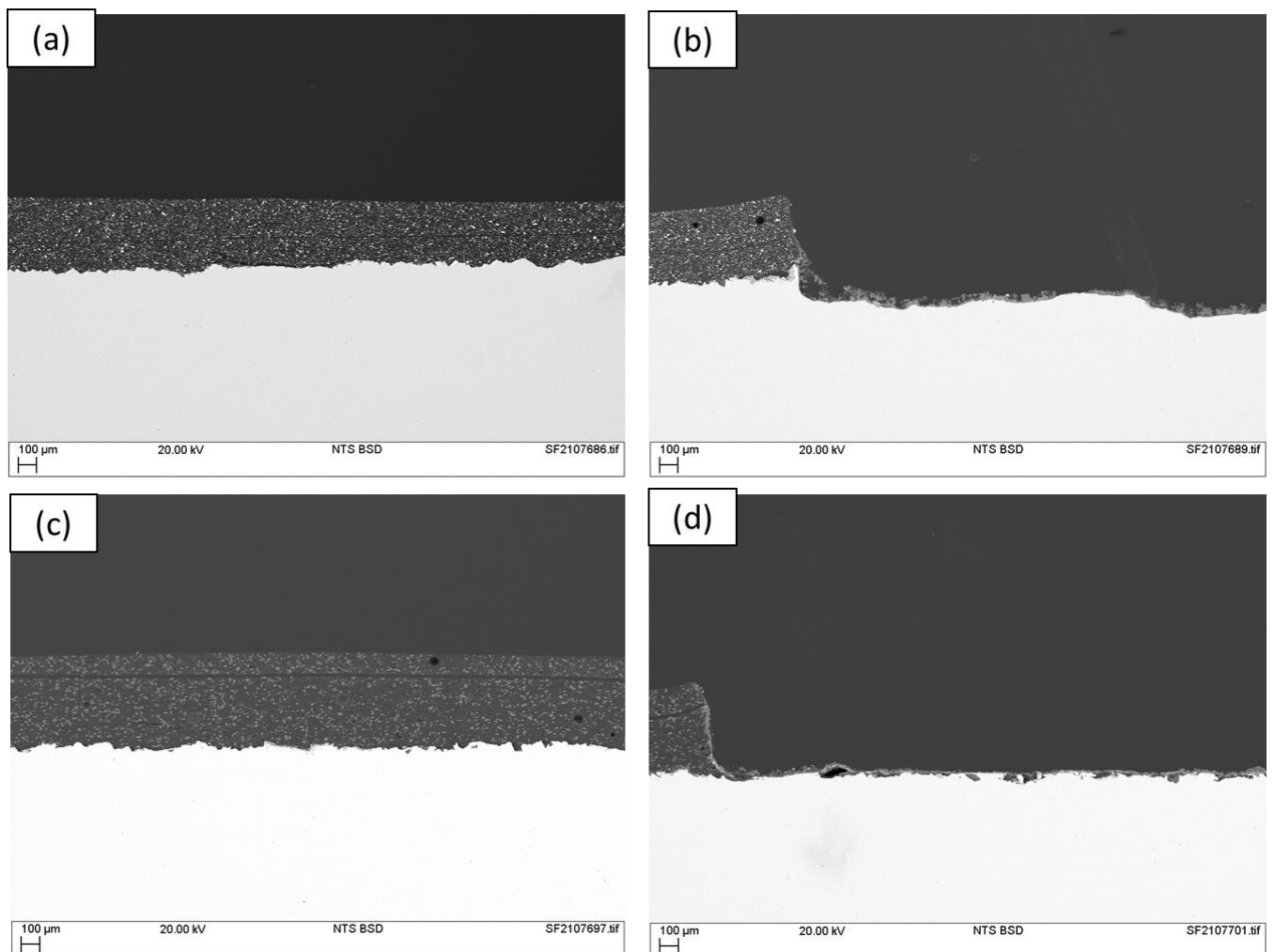
Figure 162 Cross-section of samples SA-B1 (a,b) and SA-S1 (c,d), showing the coating thickness as well as the defect area.
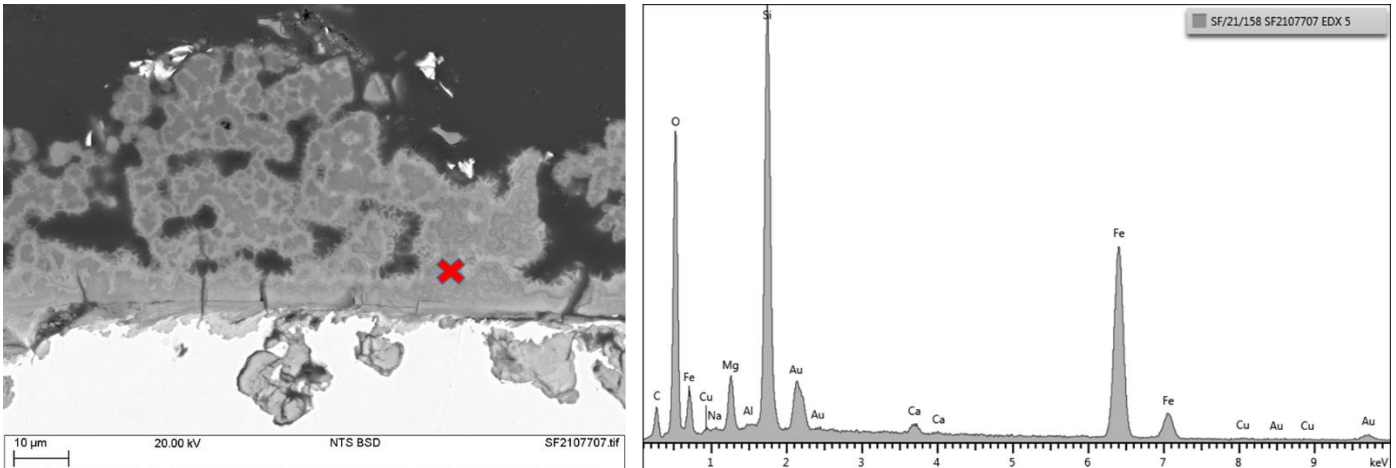
Figure 37 SEM cross-section and corresponding EDX analysis of the corrosion product on the surface of SA-B1 (carbon steel coated with Belzona 1341)
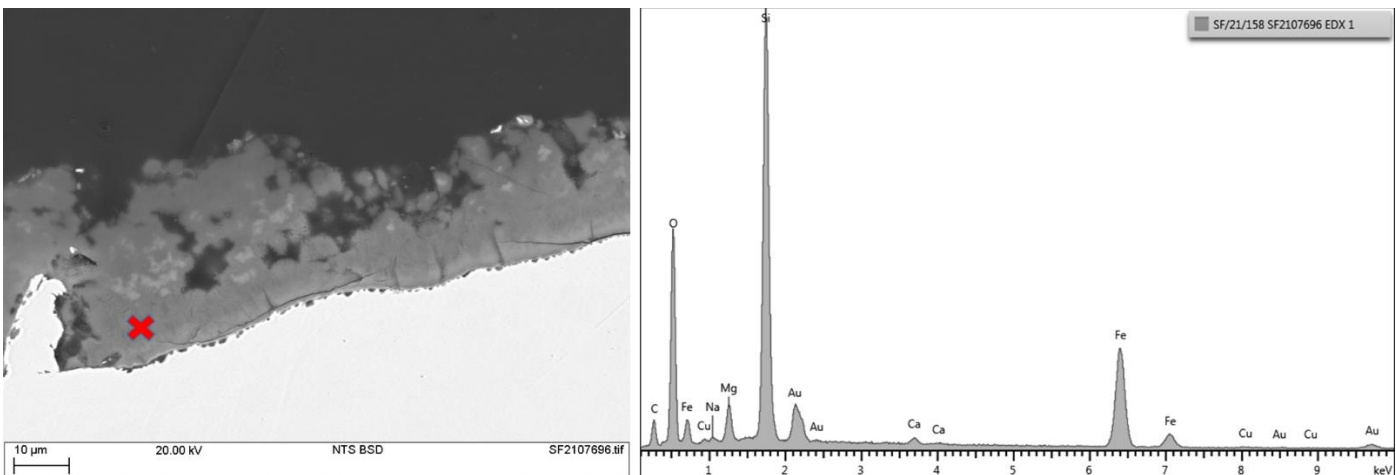
Figure 48 SEM cross-section and corresponding EDX analysis of the corrosion product on the surface of SA-S1 (carbon steel coated with Sakaphen).

5. CONCLUSIONS

In Kizildere II GPP, Zorlu Energy has implemented a design that takes care of using geothermal energy with maximum efficiency. However, while the system is working, steam flash is made three times in accordance with the design conditions and the chemical concentrations of the fluid increase [23].

With the volume capacity and retention time specified in the previous paragraph and shown in Table 2, after the scaling reactor, the silica concentration should have dropped from 451 to 265 ppm, while in the retention tank it should remain almost constant: this should occur because, having reached concentration values closer to the solubility limit, the rate of polymerization is very slow. With these conditions the retention system efficiency η_RS is expected to reach 69%. Thanks to the results of the on-site tests, we will be able to identify the optimal combination of all the parameters previously described, varying the design parameters such as pH and mass flow. In particular, the latter is a crucial parameter because it directly influences the retention time.

A review of the main parameters that affect the silica deposition has been made and a retention system for silica scaling control in geothermal applications has been developed (Appendix D). This will then be built under

WP7, as per the DoA. This approach is able to increase the plant efficiency and flexibility, guaranteeing the protection of the reinjection wells. The efficiency of the retention system gives the possibility to recover additional waste heat coupling the geothermal plant with the District Heating and/or with a low-temperature ORC. Moreover, additional economic benefits can be obtained by the sale of silica scale. The economic feasibility for Kizildere case study will be evaluated and the real effectiveness of the system will be tested using varying operational parameters, in order to validate the theoretical results. Laboratory corrosion and scaling testing of the materials for the proposed design helped to confirm the likely performance of the steel and 304L stainless steel, and the two anti-scaling coatings. Specifically, the results from the long-term U-bend SCC testing indicated that 304L was resistant to SCC in the simulated geothermal brine at pH5 and 104°C, although it was not resistant to pitting corrosion, as some small corrosion pits were observed at the end of the 29 day-long test. This was in agreement with the results from the long-term corrosion testing which indicated that both alloys suffered scaling and corrosion in the simulated geothermal brine at pH5 and 104°C. Measured based on weight change of the tested coupons, corrosion rates between 50 and 75 μm/year were measured for the tested carbon steel coatings. Furthermore, the corrosion products observed on the steel specimens suggested that the weld had not suffered preferential corrosion, which suggests that welding would not be detrimental to the corrosion performance of this material in the retention tank. Moreover, the Belzona 1341 and the Sakaphen Sakatonit Extra AR anti-scaling coatings protected the substrates from scaling and corrosion in the simulated geothermal brine at pH5 and 104°C. Therefore, from the short-term laboratory tests, these anti-scaling coatings appear suitable for the retention tank design (design temperature 104°C). Further field testing would be advisable to confirm the results presented herein.

6. APPENDICES

6.1 Appendix A

WPS for laboratory samples.

6.2 Appendix B

Results sheets for corrosion specimens.

6.3 Appendix C

Results sheets for U-bend specimens.

6.4 Appendix D

Retention Tank System Drawings for Construction:

- Scaling Reactor;
- Retention Tank;
- Overall System Plan View;
- Overall System Elevation View;

REFERENCES

[1] I. Gunnarsson, G. Ívarsson, B. Sigfússon, E.Ö. Thrastarson, G. Gíslason, *Reducing silica deposition potential in waste waters from Nesjavellir and Hellisheiði power plants, Iceland*, in Proceedings World Geothermal Congress, Bali, Indonesia (2010)

[2] M. Andhika, M.H. Castañeda, S. Regenspurg, Characterization of silica precipitation at geothermal conditions, in Proceedings World Geothermal Congress, Melbourne, Australia (2015)

[3] C. Erlindo, Jr. Angcoy, An experiment on monomeric and polymeric silica precipitation rates from supersaturated solutions, in Geothermal Training Programme, Reports 2006 Number 5

[4] D.B.van den Heuvel, E.Gunnlaugsson, I.Gunnarson, T.M.Stawski, C.L.Peacock, L.G.Benning, Understanding amorphous silica scaling under well-constrained conditions inside geothermal pipelines, in Geothermics 76 (2018) 231-241

[5] S. Arnòrsson, Environmental impact of geothermal energy utilization, in Energy, Waste, and the Environment: a Geochemical Perspective. Geological Society, London, Special Publications, 236, 297-336, (2004)

[6] T.Sugama, K.Gawlik, Anti-silica fouling coatings in geothermal environments, Material Letters, 57, issue 3 (2002)

[7] Y.Lv, M.Liu, Y.Xu, Corrosion and fouling behaviors on modified stainless steel surfaces in simulated oilfield geothermal water, Prot Met Phys Chem Surf 54, 526–535 (2018)

[8] T.Yanagase, Y.Suginohara, K.Yanagase, The properties of scales and methods to prevent them, Geothermics, Special issue 2 (1970)

[9] I.Gunnarsson, S. Arnòrsson, Treatment of geothermal waste water to prevent silica scaling, in Proceedings World Geothermal Congress, Antalya, Turkey (2005)

[10] B.Lindal, H.Kristmannsdóttir, The scaling properties of the effluent water from Kizildere Power Station, Turkey and recommendation for a pilot plant in view of district heating applications, Geothermics, 18, 217-223 (1989)

[11] I.M. Galeczka, A. Stefánsson, Chemical Composite of Kizeldere II reinjection water (2020)

[12] I.M. Galeczka, A. Stefánsson, J. Prikryl, Silica polymerization rate of re-injection water from Kizeldere II at 40-70°C, 2020

[13] F.A.Setiawan, E.Rahayuningsih, H.T.B.M.Petrus, M.I.Nurpratama, I.Perdana, Kinetics of silica precipitation in geothermal brine with seeds addition: minimizing silica scaling in a cold re-injection system, Geothermal Energy (2019) 7-22.

[14] G.A.Icopini, S.L.Brantley, P.J.Heaney, Kinetics of silica oligomerization and nanocolloid formation as a function of pH and ionic strenght at 25°C, Geochimica et Cosmochimica Acta, Vol. 69, No. 2, pp. 293-303, 2005.

[15] X.Zang, T.T.Trinh, R.A.van Santen, A.P.J.Jansen, Mechanism of the Initial Stage of Silicate Oligomerization, J. Am. Chem. Soc. 2011, 133, 6613-6625.

[16] C.F.Conrad, G.A.Icopini, H.Yasuhara, J.Z.Bandstra, S.L.Brantley, P.J.Heaney, Modeling the kinetics of silica nanocolloid formation and precipitation in geologically relevant aqueous solutions, Geochimica et Cosmochimica Acta, 71 (2007) 531-542.

[17] F.A.Setiawan, E.Rahayuningsih, H.T.B.M.Petrus, M.I.Nurpratama, I.Perdana, *Kinetics of silica precipitation in geothermal brine with seeds addition: minimizing silica scaling in a cold re-injection system*, Geothermal Energy (2019) 7-22.

[18] C.Erlindo, Jr. Angcoy, *An experiment on monomeric and polymeric silica precipitation rates from supersaturated solutions,* in Geothermal Training Programme, Reports 2006 Number 5.

[19] T. Sugama, Polyphenylenesulphide-sealed Ni-Al coatings for protecting steel from corrosion and oxidation in geothermal environments, J. Mater. Sci. 33 (1998) 3791–3803.

[20] Y. Lv, M. Liu, Y. Xu, Corrosion and Fouling Behaviors on Modified Stainless Steel Surfaces in Simulated Oilfield Geothermal Water 1, 54 (2018) 526–535.

[21] L.E. Lorensen, C.M. Walkup, E.T. Mones, UCRL-5 1843 Present status of the polymeric-materials screening program for the LLL geothermal project , 1975.

[22] ASTM International, ASTM G30 - 97(2016) - Standard Practice for Making and Using U-Bend Stress-Corrosion Test Specimens

[23] Pillai V, Kale N, Holmes B, Sabard A, Alp Sahiller H, Halacoglu U, Rouge S, Baker D, Updated End User Spec & document agreed with users, including KPI for two case study sites, Geosmart – Technologies for geothermal to enhance competitiveness in smart and flexible operation, D1.8, 2021.